MICRO-RAMAN CHARACTERIZATION OF ARSENIC-IMPLANTED SILICON: INTERPRETATION OF THE SPECTRA

JAMES P. LAVINE* and DAVID D. TUSCHEL**
*Microelectronics Technology Division, Eastman Kodak Company
Rochester, NY 14650-2008
**Imaging Research and Advanced Development, Eastman Kodak Company
Rochester, NY 14650-2017

ABSTRACT

Raman spectra were measured on arsenic-implanted silicon with micro-Raman spectroscopy in the backscattering mode and with macro-Raman spectroscopy. A peak is observed between 505 and 510 cm^{-1} with 488 and 514.5 nm excitation. This peak and a related peak from the substrate at about 520 cm^{-1} are seen in selected regions of the implanted samples when the implant dose is above 2 x 10^{14} As/cm^2. These features may be due to a long room temperature anneal, as they are absent in recently prepared samples. Possible explanations for the features are presented.

INTRODUCTION

Raman spectroscopy is used to investigate the damage caused by ion implants into semiconductors [1-3]. Generally, the extent and degree of damage grow with an increase in the implant dose. Our previous work considered the changes to the Raman spectrum of silicon caused by low-dose [4] and high-dose arsenic implants [5]. The latter reported the expected band due to amorphous silicon [6] when macro-Raman techniques were used. However, when micro-Raman spectroscopy was applied in the backscattering geometry, features were also seen at about 520 cm^{-1} and 510 cm^{-1}. Such doublets have been reported in silicon implanted with doses above 1 x $10^{16}/cm^2$ that was then laser-annealed [7,8]. The presence of the doublet was explained in terms of high electron concentrations and the expected zone-center silicon phonon. Our maximum dose is 5 x $10^{15}/cm^2$ and the samples only received room-temperature annealing, so the electron concentration is expected to be much less than the arsenic concentration. Mizoguchi et al. [9] saw a 510 cm^{-1} line in flash-lamp annealed silicon that had been implanted with 1 x 10^{15} $phosphorus/cm^2$. They associate the line with defective silicon regions that are about 1 μm in size.

Several other explanations that involve arsenic have been considered for our observed feature at about 510 cm^{-1}. Si-As vibrations occur at or below 360 cm^{-1} [10]. The observation of a line below 521 cm^{-1} line in crystalline silicon alloyed with germanium [11] appears to be related to the interdefect model [3] with Ge atoms as the "defect". The line due to Si-Ge is seen below 410 cm^{-1} [11]. Disorder-induced first-order Raman scattering usually involves zone-edge phonons, which occur below 500 cm^{-1} [12]. Resonant modes involving As atoms in Si are estimated to appear below 500 cm^{-1} with the aid of Fig. 1 of Ref. 13.

Our samples were prepared five years in advance of the Raman measurements and were first used for implanted arsenic profile determination. Whereas the above explanations for our observed Raman spectra do not seem adequate, new samples were prepared. These do not show the 510 cm^{-1} line and the 520 cm^{-1} line is not seen when the dose exceeds 5 x 10^{14} As/cm^2. The spectra of the new samples are discussed in Ref. 14. The present report proposes that the long room-temperature anneal has produced crystallites of silicon in our original samples.

Mat. Res. Soc. Symp. Proc. Vol. 588 © 2000 Materials Research Society

The second section describes the experimental details and the third section introduces typical Raman spectra for high-dose arsenic implants. The spectra are compared to calculations for the lineshapes. The final section discusses the proposed explanation for the observed Raman spectra.

EXPERIMENTAL PROCEDURES

Lightly-doped, <100>, 100-mm silicon wafers were implanted with 150 keV arsenic ions through a 0.06-μm thick thermal oxide. The arsenic dose was varied from 2×10^{13} to $5 \times 10^{15}/cm^2$ and the rate was about 1.4×10^{13} $As/s\text{-}cm^2$. The macro-Raman spectroscopy is done with a SPEX 1403 double monochromator. The samples are held in a holder such that there is a 60° angle between the incident beam and the normal to the sample surface. A 90° geometry is used for the collection of the scattered light and the incident power level is 300 mW. Micro-Raman spectroscopy is done in the back-scattering mode with the incident polarization fixed and an incident power level of 5 mW. Spectra can be collected with a polarizing filter parallel or perpendicular to the incident polarization. The sample can be rotated about the normal to the silicon surface, so Polarization /Orientation (P/O) spectra can be collected.

OBSERVATIONS AND MODELS

Figure 1 shows the macro-Raman spectra recorded when the exciting laser wavelength is 514.5 nm for a range of arsenic implant doses. Similar spectra are seen with 488 nm excitation and by Balkanski et al. [2]. The characteristic silicon optical phonon mode at 520 cm^{-1} gives way to the disorder-induced broad response below 500 cm^{-1} that is indicative of amorphous silicon (α-Si) [6]. In this case, the α-Si arises from the arsenic implant, which occupies the first 0.1 to 0.15 μm of the silicon. The residual 520 cm^{-1} line comes from the crystalline silicon below the implant-damaged silicon. Representative micro-Raman results with 514.5 nm excitation are shown in Fig. 2 for the implant dose of 5×10^{15} As/cm^2. The nearly featureless spectrum, labeled 1, has the signature of α-Si around 470 cm^{-1}. The other three spectra of Fig. 2 are from regions that show features associated with crystalline silicon (c-Si). Optical microscopy reveals these regions show contrast with the surrounding silicon when viewed with reflected white light. Their origin may be related to the long room-temperature anneal of the samples or the implantation conditions and this is discussed further in the next section.

More extensive measurements over a wide range of implant doses [5,14] show the 510 cm^{-1} feature in Fig. 2 has a tendency to grow in intensity with dose. Figures 3 and 4 illustrate this for the polarization (analyzer)/crystal orientation of parallel/0° and excitation wavelengths of 514.5 and 488 nm, respectively. This P/O setting minimizes substrate silicon contributions [15], so the silicon 520 cm^{-1} line is suppressed with 514.5 nm light and absent with 488 nm light when the arsenic dose exceeds $5 \times 10^{13}/cm^2$.

One point to note is that the 510 cm^{-1} line is present only at, and above, a dose of $2 \times 10^{14}/cm^2$, which is above the reported amorphization threshold for arsenic implants into silicon [16] at room temperature. The second point to note is that the results in Fig. 3 for 514.5 nm excitation show a peak shift with increasing dose from about 510 to 505 cm^{-1}. The 488 nm excitation results in Fig. 4 generally show a line at about 505 cm^{-1}. Finally, the 514.5 nm excitation data show an increase in the intensity of the 505 cm^{-1} feature, but this feature is sometimes absent as Fig. 2 demonstrates. The 488 nm excitation data also show an increase with dose from 2×10^{14} to 5×10^{15} As/cm^2, although the feature is absent for $5 \times 10^{14} As/cm^2$ in Fig. 4. The presence or absence of the 505 to 510 cm^{-1} feature depends on the location where the Raman measurements are made and corresponds to the different visual appearance mentioned above.

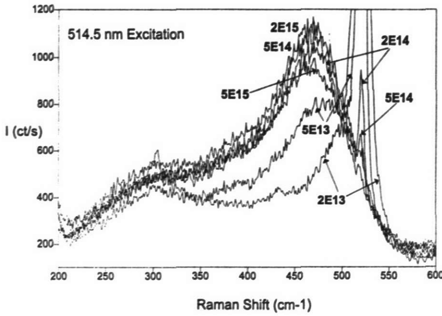

Fig. 1. Macro-Raman spectra of As-implanted Si with 514.5 nm excitation. The arsenic dose is indicated.

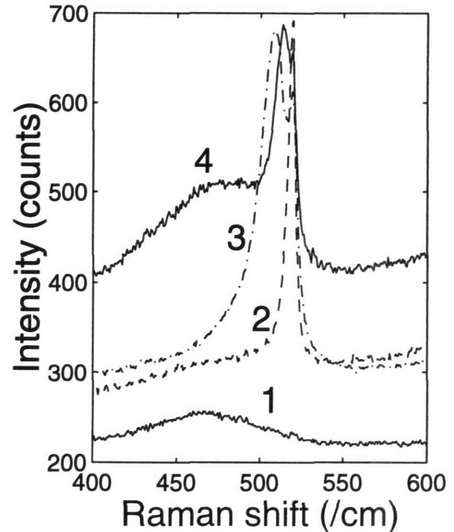

Fig. 2. Micro-Raman spectra of Si implanted with 5 x 10^{15} As/cm^2. The spectra have been shifted vertically for clarity and spectrum 3 has been multiplied by 0.5. The excitation is 514.5 nm and no analyzer is used.

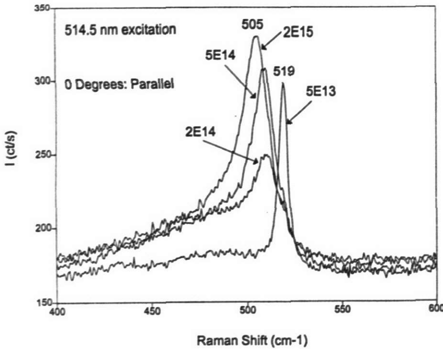

Fig. 3. Micro-Raman spectra of As-implanted Si with 514.5 nm excitation. The arsenic dose is indicated. P/O = parallel/0°.

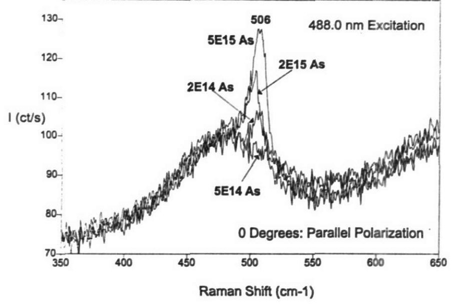

Fig. 4. Micro-Raman spectra of As-implanted Si with 488 nm excitation. The arsenic dose is indicated. P/O = parallel/0°.

Shifts of the silicon optical phonon line at 520 cm^{-1} are often interpreted in terms of the phonon confinement model (PCM) [3, 17], which accounts for the loss of crystal momentum conservation when the c-Si region size is finite. The PCM uses a weighting function such as [18]

$$W(r,L) = \sin(2\pi r/L)/[2\pi r/L] \qquad \text{if } r < L/2 \tag{1}$$

where r is the radial distance, and L is the size of the c-Si region. This W-function is set to 0 for r > L/2 and was found by Zi et al. [18] to fit the vibrational amplitude of a silicon sphere calculated with the bond polarization model. The phonon dispersion relation is also taken from Ref. 18 and is

$$\omega(q)^2 = C + D\cos(aq/4) \tag{2}$$

Here q is the crystal momentum, a is the silicon lattice constant, $C = 1.714 \times 10^5/cm^2$, and $D = 1.000 \times 10^5/cm^2$. Eq. (2) corresponds to a zone-center phonon of 521 cm^{-1}.

The Raman lineshape is proportional to $I(\omega)$, which comes from evaluating

$$I(\omega) = \int \frac{q^2 dq \sin^2(qL/2) / [q^2(4\pi^2 - q^2L^2)^2]}{\{[\omega - \omega_s - \omega(q)]^2 + (\Gamma_0/2)^2\}} \tag{3}$$

where $\Gamma_0 = 3$ cm^{-1}, ω_s represents a shift due to stress, and q goes from 0 to $2\pi/a$. Figure 5 with $\omega_s = 0$ shows the lineshift of the 520 cm^{-1} line and its full width at half maximum (FWHM) as a function of L for Eqs. 1 to 3. Figure 6 compares the predicted lineshapes with spectra 3 and 4 of Fig. 2. Scaled versions of spectrum 1 of Fig. 2 are subtracted from the other experimental spectra to remove the α-Si peak near 480 cm^{-1}. The resulting spectrum 2 is then subtracted from spectra 3 and 4 to remove the substrate contribution at 520 cm^{-1}. Spectra 3 and 4 are then shifted vertically and plotted in Fig. 6. For a specified lineshift, the experimental linewidths are smaller than the model's predictions, so the linewidth is used to predict the L. The lineshift is adjusted through the use of a non-zero ω_s, which is attributed to stress [3,9]. It is apparent that if c-Si structures are present, then they are about 19 to 30 Å in size and a tensile stress exists. The lines from Figs. 3 and 4 agree with these fits.

DISCUSSION

The last section shows that the implanted samples with a strong Raman response between 505 and 510 cm^{-1} are consistent with the presence of small crystalline regions. The existence of these c-Si regions requires an explanation. It has been reported that high-dose implants may not render the implanted area completely amorphous [19]. Since increased doses should leave fewer c-Si regions, the intensity of the ~510 cm^{-1} line should decrease with dose. This is opposite to the observed trend, so another explanation is sought. A lower dose in particular areas may also lead to silicon crystallites. This seems unlikely with implants on a production ion implanter and would appear less likely as the dose increases. Yet the c-Si regions are seen on the highest dose implanted sample.

Room-temperature annealing over nearly five years is postulated to provide the thermal treatment necessary to convert limited regions of α-Si to c-Si. Perhaps a higher dose of arsenic leads to more nucleation sites. This would explain the increased intensity of the 505 to 510 cm^{-1} lines with increased implant dose. It is known that arsenic or phosphorus does enhance the rate

Fig. 5. Model calculations of the lineshift and the full width at half maximum versus the crystallite size.

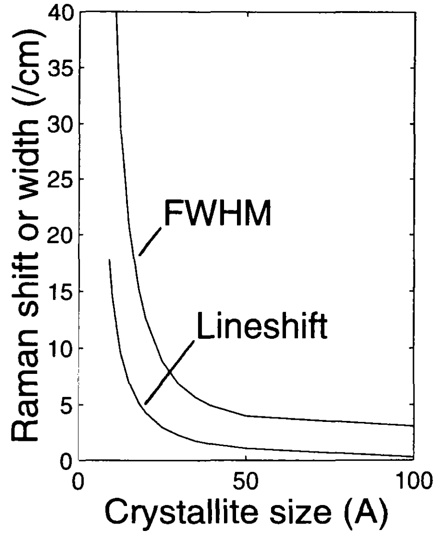

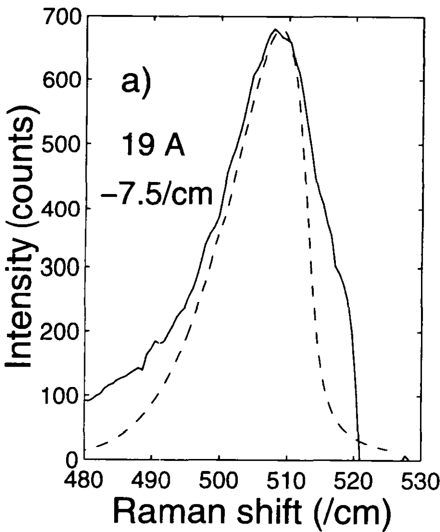

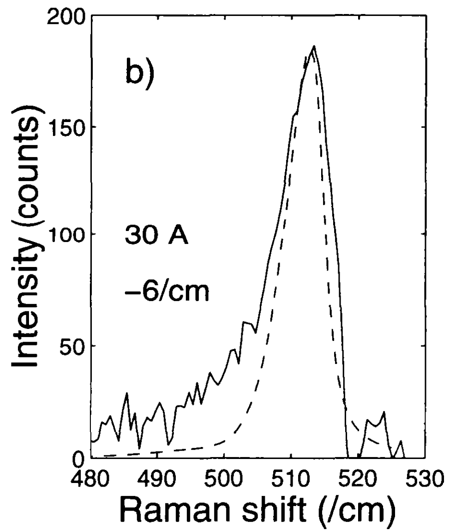

Fig. 6. Comparisons of model (dashed lines) with micro-Raman spectra (solid lines) a) 3 and b) 4 from Fig. 2. The dose is 5 x 10^{15} As/cm^2. The α-Si and substrate contributions have been subtracted from the data. The model values of L and ω_s are indicated.

of solid phase epitaxial regrowth in implanted silicon [20]. However, a straightforward extrapolation of the recrystallization velocity data from 475 to 525°C to room temperature leads to about 4 x 10^{-25} Å /s. This is clearly inadequate to explain the present data. Ion implantation-

induced point defects and some of their complexes do undergo annealing at room temperature [21]. It is possible this leads to the formation of small regions of c-Si as the time scales for the defect annealing [22] are compatible with our five years at room temperature.

The indication is that the original samples have "relaxed" with time and show very small regions of c-Si. Other ways to explore the extent of crystallinity and the presence of stress in the original samples are under consideration.

ACKNOWLEDGEMENTS

We thank Jean Catone, Hung Doan, and Paul Whalen for the ion implants and S.-Tong Lee for the secondary ion mass spectroscopy analysis of the arsenic profiles. We also thank Prof. Jose Menendez and Dr. John Spoonhower for their useful suggestions.

REFERENCES

1. G. Braunstein, D. Tuschel, S. Chen, S.-T. Lee, J. Appl. Phys. **66**, 3515 (1989).
2. M. Balkanski, J.F. Morhange, G. Kanellis, J. Raman Spectros. **10**, 240 (1981).
3. X. Huang, F. Ninio, L.J. Brown, S. Prawer, J. Appl. Phys. **77**, 5910 (1995).
4. D.D. Tuschel, J.P. Lavine, J.B. Russell, in *Diagnostic Techniques for Semiconductor Materials Processing II*, edited by S.W. Pang, O.J. Glembocki, F.H. Pollak, F.G. Celii, and C.M. Sotomayor Torres (Mater. Res. Soc. Symp. Proc. **406**, Pittsburgh, PA, 1996) pp. 549-554.
5. J.P. Lavine and D.D. Tuschel, Bull. Am. Phys. Soc. **44**, 1338, paper SC08-8 (1999).
6. J.S. Lannin, Semiconductors and Semimetals **21**, Part B, Ch. 6 (1984).
7. A.K. Shukla and K.P. Jain, Phys. Rev. B **34**, 8950 (1986).
8. G. Contreras, A.K. Sood, M. Cardona, A. Compaan, Solid State Commun. **49**, 303 (1984).
9. K. Mizoguchi, H. Harima, S.-i. Nakashima, T. Hara, J. Appl. Phys. **77**, 3388 (1995).
10. R.J. Nemanich and J.C. Knights, J. Non-Crystall. Solids **35/36**, 243 (1980).
11. W.J. Brya, Solid State Commun. **12**, 253 (1973).
12. R.A. Forman, M.I. Bell, D.R. Myers, D. Chandler-Horowitz, Japan. J. Appl. Phys. **24**, L848 (1985).
13. A.A. Maradudin, Solid State Phys. **18**, 273 (1966).
14. D.D. Tuschel and J.P. Lavine, this Proceedings.
15. P.Y. Yu and M. Cardona, *Fundamentals of Semiconductors, Physics and Materials Properties*, 2nd ed. (Springer, Berlin, 1999), p. 368.
16. F.F. Morehead, Jr. and B.L. Crowder, in *Ion Implantation*, edited by F.H. Eisen and L.T. Chadderton (Gordon and Breach, London, 1971), pp. 25-30.
17. H. Richter, Z.P. Wang, L. Ley, Solid State Commun. **39**, 625 (1981).
18. J. Zi, K. Zhang, X. Xie, Phys. Rev. B **55**, 9263 (1997).
19. Y. Komem and I.W. Hall, J. Appl. Phys. **52**, 6655 (1981).
20. L. Csepregi, E.F. Kennedy, T.J. Gallagher, J.W. Mayer, T.W. Sigmon, J. Appl. Phys. **48**, 4234 (1977).
21. J. Bourgoin and M. Lannoo, *Point Defects in Semiconductors II* (Springer-Verlag, Berlin, 1983), ch. 9.
22. F.L. Vook and H.J. Stein, Radiat. Eff. **2**, 23 (1969).